

LETTER TO THE EDITOR

Advanced precision modeling reveals divergent responses of hepatocellular carcinoma to combinatorial immunotherapy

Dear Editor

Combinatorial immunotherapy has provided patients with advanced hepatocellular carcinoma (HCC) the potential for long-term survival. However, sustained responses are seen only in a minority of patients [1]. Thus, there is an unmet need for precision modeling to understand the different responses and uncover predictive biomarkers for treatment stratification.

Here, we investigated the responses of HCC to combinatorial immunotherapy in two genetic mouse models, N90-CTNNB1^{OE};TP53^{KO} and Myc^{OE};TGF α ^{OE} mice, which produce overexpression of an activated form of β -catenin (CTNNB1) together with deletion of tumor protein 53 (TP53) or overexpression of the MYC oncogene together with transforming growth factor α (TGF α), respectively. Mutations in these pathways are frequently present in human HCC. We found that the two models of HCC displayed remarkably distinct immune landscapes (Figure 1A, Supplementary Figures S1–S2). Multi-locular tumors developed rapidly (less than 3 months) in both models (Figure 1A, Supplementary Figure S1E). Remarkably, the Myc-driven Myc^{OE};TGF α ^{OE} tumors were immunologically “cold” and exhibited high proliferation rates, while N90-CTNNB1^{OE};TP53^{KO} tumors were immunologically “hot” and showed elevated levels of vascularization and immune cell infiltration (Supplementary Figures S1–S2).

Given the increased expression of vascular endothelial growth factor (VEGF) and programmed cell death-ligand 1 (PD-L1) in the N90-CTNNB1^{OE};TP53^{KO} model (Supplementary Figure S2), we investigated if there are distinct responses of the two HCC models to combi-

natorial immunotherapy. We administered lenvatinib, a multi-tyrosine kinase inhibitor that inhibits both the VEGF and tumor fibroblast growth factor receptor pathways together with anti-programmed cell death protein 1 (PD-1) antibodies to N90-CTNNB1^{OE};TP53^{KO} or Myc^{OE};TGF α ^{OE} mice with fully established tumors (Supplementary Figure S3A). Remarkably, the combinatorial immunotherapy significantly reduced the burden of large tumors (≥ 2 mm-size) compared with IgG isotype control in N90-CTNNB1^{OE};TP53^{KO} animals, but not in the Myc^{OE};TGF α ^{OE} -driven model (Figure 1A, Supplementary Figure S3). Thus, immunologically “hot” N90-CTNNB1^{OE};TP53^{KO} tumors responded more to combinatorial immunotherapy than immunologically “cold” Myc^{OE};TGF α ^{OE} tumors.

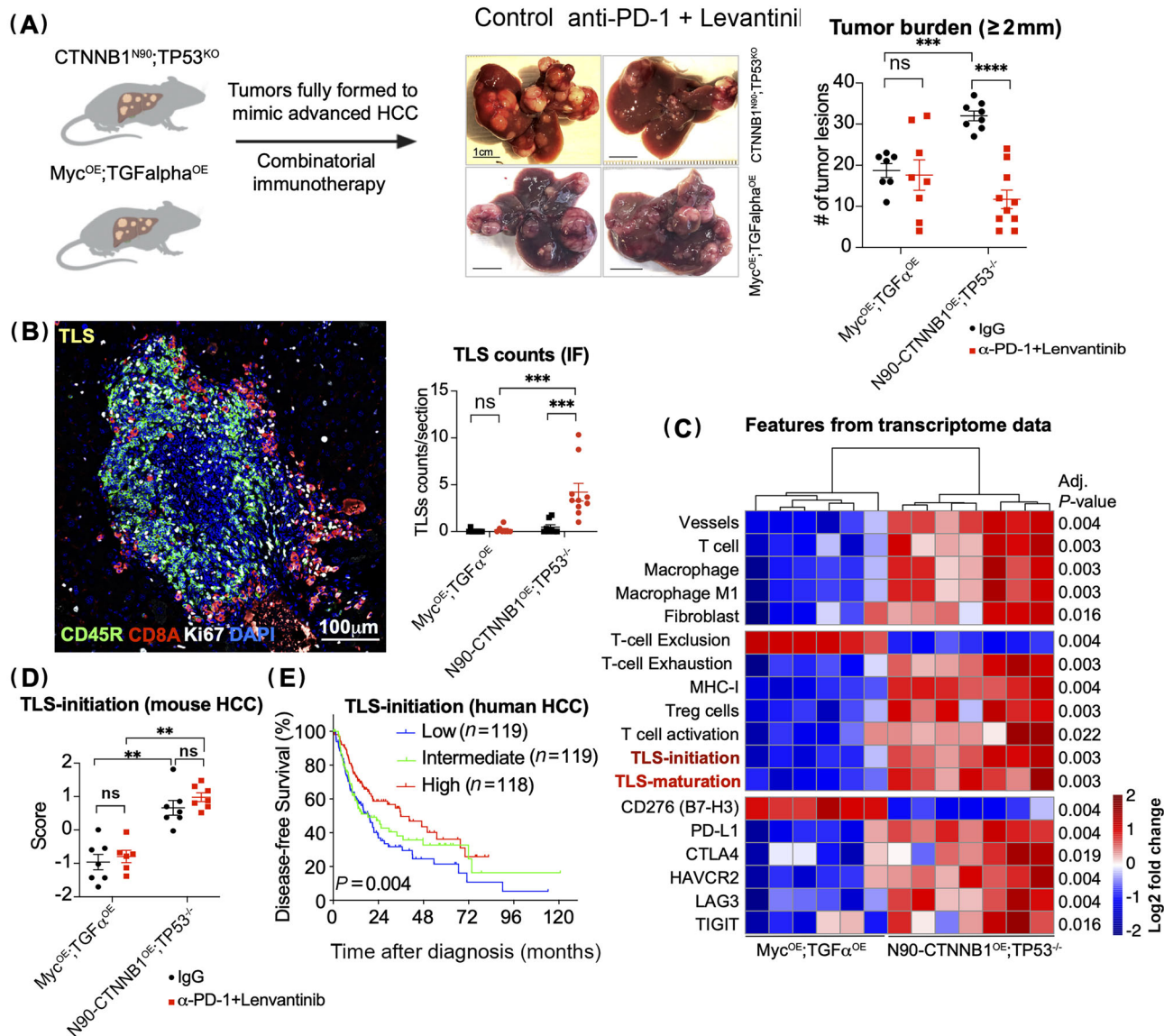
Next, we investigated the hepatic response to combinatorial immunotherapy in both models in detail by immunofluorescence staining with the B cell marker CD45R and the CD8⁺ T marker CD8A in combination with Ki67 to assess proliferation and T and B cell activation status. Strikingly, we found that immune cell clusters in the N90-CTNNB1^{OE};TP53^{KO} model contained tertiary lymphoid structures (TLSs) with B cell follicle and T cell zones after combinatorial immunotherapy (Figure 1B; Supplementary Figure S4). Notably, of the 93 TLSs observed in our study, 88 were located in the tumor periphery, while only 5 were present within the tumor itself (data not shown). A large proportion of follicular B cells were Ki67 positive (74.8% for treatment versus 27.8% for IgG isotope control) in TLSs of CTNNB1^{OE};TP53^{KO} mice, indicating their high activation state (data not shown). In contrast, the Myc/TGF α -driven tumors exhibited very few TLSs (Figure 1B). Collectively, the less proliferative N90-CTNNB1^{OE};TP53^{KO} tumors were responsive to combinatorial immunotherapy, which was associated with an augmented TLS response.

To better understand the distinct responses of the two HCC models to combinatorial immunotherapy, we employed NanoString technology to perform immune transcriptomic profiling of N90-CTNNB1^{OE};TP53^{KO}- and

Abbreviations: HCC, Hepatocellular Carcinoma; TLS, Tertiary lymphoid structures; TGF α , transforming growth factor alpha; CTNNB1, gene encoding beta-catenin; PD-1, programmed cell death protein 1; IgG, immunoglobulin G (control); IF, immunofluorescence; PD-L1, programmed cell death protein 1 ligand; MHC-I, major histocompatibility complex class I; Treg, regulatory T cell; CTLA4, cytotoxic T-lymphocyte-associated protein 4; HAVCR2, hepatitis A virus cellular receptor 2; LAG3, lymphocyte-activation gene 3; TIGIT, T cell immunoreceptor with Ig and ITIM domains.

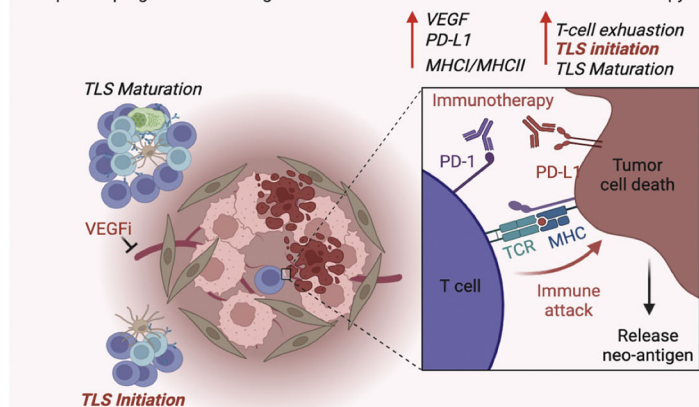
This is an open access article under the terms of the [Creative Commons Attribution-NonCommercial-NoDerivs](https://creativecommons.org/licenses/by-nc-nd/4.0/) License, which permits use and distribution in any medium, provided the original work is properly cited, the use is non-commercial and no modifications or adaptations are made.

© 2023 The Authors. *Cancer Communications* published by John Wiley & Sons Australia, Ltd. on behalf of Sun Yat-sen University Cancer Center.



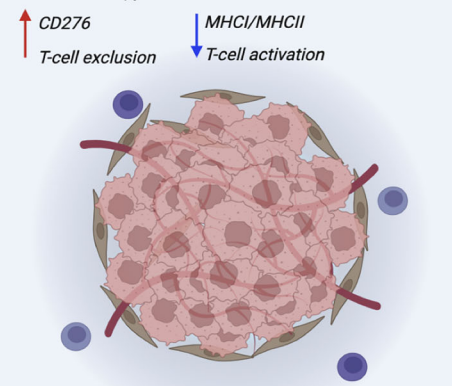
(F) HCC Hot Tumor Model

- Less proliferative cancer cell
- T cell exhaustion, elevated PD-1/PD-L1, aggregated CD8+ T cells/B cells
- Improved prognosis and killing of tumor cells with the combinatorial immunotherapy



HCC Cold Tumor Model

- Highly proliferative cancer cells
- T cell exclusion
- Poor prognosis and response to the combinatorial immunotherapy



Myc^{OE};TGF α ^{OE}-driven tumors with or without combinatorial immunotherapy. Notably, the expression of genes relevant to the TLS response was highly elevated in the N90-CTNNB1^{OE};TP53^{KO}-driven tumor model (Figure 1C, Supplementary Figure S5).

We next focused on ten differentially expressed TLS genes previously recognized as crucial for TLS formation, maturation, or both [2–8]. Among these genes are B-cell lymphoma 6 (*Bcl6*), myocyte-specific enhancer factor 2C (*Mef2c*), and chemokine [C-X-C motif] ligand 13 (*Cxcl13*) (Supplementary Figure S5D and S5F), which are markers of TLS, while the seven other genes have been implicated in TLS initiation. Next, we derived TLS-maturation and TLS-initiation scores based on the expression levels of these genes and found both to be significantly higher in N90-CTNNB1^{OE};TP53^{-/-} versus Myc^{OE};TGF α ^{OE} samples prior to and post combinatorial immunotherapy (Figure 1D, Supplementary Figure S5E). Thus, increased TLS initiation and maturation in the livers of N90-CTNNB1^{OE};TP53^{-/-} mice were associated with their higher sensitivity to combinatorial immunotherapy.

Among the TLS genes, only *Bcl6*, a master regulator for germinal center maturation, and *Cxcl13*, a marker gene for activated TLS [7], exhibited increased mRNA expression after combinatorial immunotherapy in the N90-CTNNB1^{OE};TP53^{KO} model (Supplementary Figure S5F). When we evaluated how the activation of these two genes relates to TLS activation, we found that *Bcl6* was positively correlated with TLS activation, while the opposite was true for *Cd276* (Supplementary Figure S5G). Next, we

investigated human HCC gene expression data and discovered a highly significant, positive correlation between *CTNNB1* and *BCL6* ($r = 0.527$, $P < 0.001$) or *MEF2C* transcript levels ($r = 0.504$, $P < 0.001$) (Supplementary Figure S5H), and a highly significant, positive correlation between hypoxia-inducible factor (*HIF1A*) and *BCL6* ($r = 0.405$, $P < 0.001$) (Supplementary Figure S5I). HIF1A-binding motif analysis suggested that HIF1A bound specifically to the *BCL6* promoter (Supplementary Figure S5J-K). Taken together, these results demonstrate that TLS gene signatures are distinguishing features of the immunologically hot N90-CTNNB1^{OE};TP53^{-/-} model.

Finally, we examined which gene ontology pathways are significantly enriched in response to combinatorial immunotherapy. Not surprisingly, we found that pathways such as adaptive and innate immune responses, TNF signaling, IFN- γ and NF- κ B signaling, among others, were significantly enriched (Supplementary Figure S6A). To assess if T-cell exhaustion and T-cell exclusion associate with response and resistance to combinatorial immunotherapy, we derived gene sets to compute T-cell exhaustion and T-cell exclusion scores. When we analyzed features from our transcriptome data that differentiate the two genetic models post combinatorial immunotherapy, we found that expression of *Cd276* and the T-cell exclusion gene signature were enriched in the tumor microenvironment of the immunologically cold Myc^{OE};TGF α ^{OE} model compared to the CTNNB1^{OE};TP53^{KO} model (Figure 1C). However, all other features, including the aforementioned TLS initiation and

FIGURE 1 Combinatorial immunotherapy has distinct effects in immunologically “hot” N90-CTNNB1^{OE};TP53^{-/-} and “cold” Myc^{OE};TGF α ^{OE} models of HCC. (A) **Left panel:** Schematic N90-CTNNB1^{OE};TP53^{-/-} and Myc^{OE};TGF α ^{OE} mouse models with fully formed HCC lesions were treated with anti-PD-1 plus lenvatinib. Anti-IgG isotype and buffer were used in control groups. **Middle panel:** Representative images of liver tissues and H&E staining of sections after anti-PD-1 plus lenvatinib treatment or control in the two mouse models as indicated. **Right panel:** Quantitation of tumor lesions with a diameter of ≥ 2 mm in the two mouse models with anti-PD-1 plus lenvatinib treatment and control as indicated (8–10 mice per group). (B) **Left panel:** Immunofluorescence staining for immune cells and proliferation markers CD45R, CD8A, Ki67 of a peritumor tertiary lymphoid structure (TLS) in the liver of a N90-CTNNB1^{OE};TP53^{-/-} mouse. **Right panel:** Quantification of TLS counts using immuno-staining data from liver sections of N90-CTNNB1^{OE};TP53^{-/-} and Myc^{OE};TGF α ^{OE} mice. Black circles, IgG control; red squares, treatment with anti-PD-1 and Lenvatinib. (8–10 mice per group, one section each). Mean and SEM are shown. Mann-Whitney test. $**P < 0.01$, $***P < 0.001$. (C) Transcriptomic features in immunologically “hot” vs. “cold” tumor models. Note that the immunologically “cold” Myc^{OE};TGF α ^{OE} tumors are highly enriched for T cell exclusion features and exhibit high expression of CD276, which is an immune checkpoint molecule that inhibits tumor antigen-specific immune responses. In contrast, immunologically “hot” CTNNB1^{OE};TP53^{-/-} tumors are highly enriched for all other features, including TLS initiation and maturation and MHC class I expression. (D) TLS initiation scores derived from liver tumor transcriptome data were used to analyze TLS in the tumor models with or without treatment as indicated. Adjusted P values are obtained from Benjamini-Hochberg correction of Mann-Whitney test. (E) Kaplan-Meier survival analysis of the TCGA LIHC cohort using the TLS initiation score derived from our mouse data stratified into tertiles. The P value indicates a significant difference between patients with high and low TLS initiation scores. (F) Schema summarizing the features of immunologically “hot” and “cold” tumors which are exemplified by our two genetic precision models of HCC. Abbreviations: HCC, hepatocellular carcinoma; PD-1, programmed cell death protein 1; IgG, immunoglobulin G (control); TLS, tertiary lymphoid structure; IF, immunofluorescence; PD-L1, programmed cell death protein 1 ligand; MHC-I, major histocompatibility complex class I; Treg, regulatory T cell; CTLA4, cytotoxic T-lymphocyte-associated protein 4; HAVCR2, hepatitis A virus cellular receptor 2; LAG3, lymphocyte-activation gene 3; TIGIT, T cell immunoreceptor with Ig and ITIM domains.

maturation scores and the T-cell exhaustion scores, were enriched in the CTNNB1^{OE};TP53^{KO} model, both prior to and post combinatorial immunotherapy (Figure 1C, Supplementary Figure S6B).

Next, we performed disease-free survival analysis in human HCC patients stratified by the TLS initiation scores calculated using gene expression data. As shown in Figure 1E, high TLS initiation scores were significantly associated with longer disease-free survival. Conversely, low T-cell exclusion scores predicted longer disease-free survival (Supplementary Figure S6C). A model summarizing our findings is shown in Figure 1F. In sum, liver cancer driven by activation of the β -catenin pathway and loss of p53 (the CTNNB1^{OE};TP53^{KO} model) is an example of immunologically “hot” HCC, which benefits significantly from combinatorial immunotherapy. The TLS-related features we derived from transcriptomics data can predict the efficacy of combinatorial immunotherapy, while immune exclusion predicts immunotherapy failure, exemplified by the highly proliferative but treatment-resistant Myc^{OE};TGF α ^{OE} model. Thus, our study suggests that future stratification based on TLS and T cell exclusion features prior to treatment can predict the response to combinatorial immunotherapy.

DECLARATIONS

AUTHOR CONTRIBUTIONS

Jinping Liu: Investigation, Visualization, Writing-Original draft; Lan Cheng: Investigation; Hilana El-Mekkoussi: Investigation; Charles-Antoine Assenmacher: Formal analysis; Michelle Y. Y. Lee: Formal analysis; Danielle R. Jaffe: Investigation; Kaisha Garvin-Darby: Investigation; Ashleigh Morgan: Investigation; Elisabetta Manduchi: Formal Analysis; Jonathan Schug: Formal analysis; Klaus H. Kaestner: Writing – Original Draft, Funding acquisition, Supervision.

ACKNOWLEDGMENTS

We thank Drs. S. Shapira (University of Pennsylvania) and K. Wangenstein (Mayo Clinic) for critical reading of the manuscript. We also thank D. Getz, L. Robillard, Drs. R. Dusek and W. Wu (University of Pennsylvania) for the suggestions of administering Lenvatinib and anti-PD-1 combinatorial immunotherapy.

CONFLICTS OF INTERESTS STATEMENT

The authors declare that they have no competing interests.

FUNDING INFORMATION

This work was supported by the National Institutes of Health grant R01-CA-249929-06A1 to KHK. We acknowledge support from the Molecular Pathology & Imaging

Core (MPIC) of the UPenn Center for Molecular Studies in Digestive and Liver Diseases (P30 DK050306), the Comparative Pathology Core, the Wistar Institute Genomics Facility, the Functional Genomics Core of the UPenn Diabetes Research Center (P30 DK019525).

ETHICS APPROVAL

Animal studies were approved by the Institutional Animal Care and Use Committee of the University of Pennsylvania under protocol # 805623.

CONSENT FOR PUBLICATION

Not applicable.

DATA AVAILABILITY STATEMENT

Plasmids used for the derivation of the mouse models are available upon request.

Jinping Liu¹

Lan Cheng²

Hilana El-Mekkoussi¹ 


Charles-Antoine Assenmacher³

Michelle Y. Y. Lee¹

Danielle R. Jaffe¹

Kaisha Garvin-Darby¹

Ashleigh Morgan¹

Elisabetta Manduchi¹ 

Jonathan Schug¹

Klaus H. Kaestner¹ 

¹Department of Genetics and Center for Molecular Studies in Digestive and Liver Disease, University of Pennsylvania, Philadelphia, PA, USA

²Institute for Diabetes, Obesity and Metabolism, Perelman School of Medicine at the University of Pennsylvania, Philadelphia, PA, USA

³Department of Pathobiology, School of Veterinary Medicine, University of Pennsylvania, Philadelphia, PA, USA

Correspondence

Klaus H. Kaestner, PhD, MS, Department of Genetics and Center for Molecular Studies in Digestive and Liver Disease, University of Pennsylvania, Philadelphia, PA, 19104, USA.

Email: kaestner@penntmedicine.upenn.edu

ORCID

Hilana El-Mekkoussi  <https://orcid.org/0000-0001-5561-4358>

Elisabetta Manduchi  <https://orcid.org/0000-0002-4110-3714>

Klaus H. Kaestner  <https://orcid.org/0000-0002-1228-021X>

REFERENCES

1. Finn RS, Qin S, Ikeda M, Galle PR, Ducreux M, Kim TY, et al. Atezolizumab plus bevacizumab in unresectable hepatocellular carcinoma. *N Engl J Med.* 2020;382(20):1894–905.
2. Basso K, Saito M, Sumazin P, Margolin AA, Wang K, Lim WK, et al. Integrated biochemical and computational approach identifies bcl6 direct target genes controlling multiple pathways in normal germinal center b cells. *Blood.* 2010;115(5):975–84.
3. Buckley CD, Barone F, Nayar S, Benezech C, Caamano J. Stromal cells in chronic inflammation and tertiary lymphoid organ formation. *Annu Rev Immunol.* 2015;33:715–45.
4. Chen SC, Vassileva G, Kinsley D, Holzmann S, Manfra D, Wiekowski MT, et al. Ectopic expression of the murine chemokines ccl21a and ccl21b induces the formation of lymph node-like structures in pancreas, but not skin, of transgenic mice. *J Immunol.* 2002;168(3):1001–8.
5. De Silva NS, Klein U. Dynamics of B cells in germinal centres. *Nat Rev Immunol.* 2015;15(3):137–48.
6. Dent AL, Shaffer AL, Yu X, Allman L, Staudt LM. Control of inflammation, cytokine expression, and germinal center formation by bcl-6. *Science.* 1997;276(5312):589–92.
7. Havenar-Daughton C, Lindqvist M, Heit A, Wu JE, Reiss SM, Kendric K, et al. Cxcl13 is a plasma biomarker of germinal center activity. *Proc Natl Acad Sci U S A.* 2016;113(10):2702–7.
8. Johansson-Percival A, He B, Li ZJ, Kjellen A, Russell K, Li J, et al. De novo induction of intratumoral lymphoid structures and vessel normalization enhances immunotherapy in resistant tumors. *Nat Immunol.* 2017;18(11):1207–17.

SUPPORTING INFORMATION

Additional supporting information can be found online in the Supporting Information section at the end of this article.